Supplementary Materials

Hanchen Xu[1,#], Hongwei Shou[1,#], Quan Zhou[1], Hengjie Liu[1], Shiqiang Wei[1], Xiaojun Wu[2,*], Changda Wang[1,*], Li Song[1,3,*]

[1]National Synchrotron Radiation Laboratory, CAS Center for Excellence in Nanoscience, University of Science and Technology of China, Hefei 230029, Anhui, China.
[2]CAS Key Laboratory for Materials for Energy Conversion, School of Chemistry and Materials Science, Synergetic Innovation of Quantum Information & Quantum Technology, University of Science and Technology of China, Hefei 230026, Anhui, China.
[3]Zhejiang Institute of Photonelectronics, Jinhua 321004, Zhejiang, China.
[#]Authors contributed equally to this work.

[*]**Correspondence to:** Prof. Xiaojun Wu, CAS Key Laboratory for Materials for Energy Conversion, School of Chemistry and Materials Science, Synergetic Innovation of Quantum Information & Quantum Technology, University of Science and Technology of China, Hefei 230026, Anhui, China. E-mail: xjwu@ustc.edu.cn; Prof. Changda Wang, Prof. Li Song, National Synchrotron Radiation Laboratory, CAS Center for Excellence in Nanoscience, University of Science and Technology of China, Hefei 230029, Anhui, China. E-mail: wchda@ustc.edu.cn; song2012@ustc.edu.cn

This PDF file includes:

Experimental Section

Materials Characterization: X-ray diffraction (XRD) patterns of the samples were obtained using a multipurpose rotating target X-ray diffractometer with a Cu K_α radiation source (λ = 1.54178 Å). Morphological characterization Scanning Electron Microscope (SEM) and Energy-Dispersive X-ray Spectroscopy (EDS) was performed using an SU8220 cold field emission scanning electron microscope (15 kV, JEOL, JSM-6700F). X-ray photoelectron spectroscopy (XPS) results were acquired from an ESCALAB 250Xi spectrometer. Mo K-edge X-ray absorption spectra were collected in transmission/fluorescence mode at the 1W1B beamline of the Beijing Synchrotron Radiation Facility (BSRF, Beijing). During the measurements, the X-rays were monochromatized by a Si(111) double-crystal monochromator. Additionally, the position of the absorption edge was calibrated using Mo foil. All measurement data for ex situ X-ray absorption fine structure (XAFS) were collected within one period. Spectral analysis was performed using the Athena software[1].

Electrochemical Measurements: Electrochemical tests were performed using a CH660D electrochemical workstation with a three-electrode system, employing the prepared samples as the working electrode, a carbon rod as the counter electrode, and Ag/AgCl (3M KCl) as the reference electrode. The glassy carbon working electrode was prepared by dispersing 2 mg of the sample in a solution containing 750 μL of water, 250 μL of isopropanol, and 30 μL of Nafion solution, followed by 30 min of sonication. A 10 μL aliquot of the mixed solution was then drop-cast onto the surface of the glassy carbon electrode (3 mm diameter) and dried at 60°C for 2 h. Cyclic voltammetry (CV) curves were recorded at various scan rates, and galvanostatic charge-discharge curves (GCD) were measured at different current densities within a voltage window of -0.1-0.4 V. All electrochemical tests were conducted at room temperature in a 1 M H_2SO_4 electrolyte.

Computational Details: This study jointly uses VASP[2] and JDFTx[3]. The former is used for structural optimization and electronic structure calculations, while the latter is utilized to compute properties related to the double layer[4, 5]. The Vienna Ab initio Simulation Package (VASP) utilizes density functional theory (DFT) calculations

applying the Perdew-Burke-Ernzerhof (PBE) formulation within the generalized gradient approximation (GGA) [6]. Ion cores are characterized using projected augmented wave (PAW) potentials, and a plane wave basis set with a 450 eV kinetic energy cutoff accounts for valence electrons[7]. Gaussian smearing allows for partial occupancies of Kohn-Sham orbitals with a width parameter of 0.05 eV.

Self-consistent electronic energy requires an energy fluctuation less than 0.01 eV/Å. The Brillouin zone employs a 7×4×1 k-point grid, and self-consistent field (SCF) calculations operate with an energy of 1×10^{-8} eV. Convergence in geometry optimization is achieved once the energy change falls below a defined threshold. To obtain a more accurate electronic structure, a 19 × 11 × 1 k-point grid is utilized. A vacuum of at least 15 Å exists perpendicular to the surface in all systems.

JDFTx employs the GGA-PBEsol functional to describe exchange-correlation energy. The ultrasoft pseudopotential characterizes the interaction between atomic nuclei and electrons. The kinetic energy cutoff is defined at 20 Hartree. The implicit electrolyte is modeled by the linear polarizable continuum model (LinearPCM) coupled with the CANDLE model in a 1M NaF solution to capture solvation effects and the electrolyte response to surface net charge[8].

The quantum capacitance is calculated using the fixed-band approximation, as per the following formula[4, 9]:

$$C_Q=\frac{dQ}{d\varphi}=\frac{e^2}{4KT}\int_{-\infty}^{+\infty} D(E)sech^2\left[\frac{E-\varphi}{2kT}\right]dE \qquad (1)$$

here, $D(E)$ represents the density of states, and φ is the applied potential.

The double-layer potential is calculated by determining the shift in the Fermi energy level within a unit voltage, as per the following formula[10, 11]:

$$C_{EDL}=\Delta\sigma/\Delta E \qquad (2)$$

where $\Delta\sigma$ represents the surface charge density and ΔE represents the relative displacement of the Fermi level.

Then, using the same surface charge Q, the corresponding φ_Q and φ_{EDL} are obtained. In the case of two capacitors in series, $\varphi_{Tot}=\varphi_Q+\varphi_{EDL}$, implying that the total capacitance $C_{Tot}=Q/\varphi_{Tot}$ is equal to $1/C_{Tot}=1/C_Q+1/C_{EDL}$.[11]

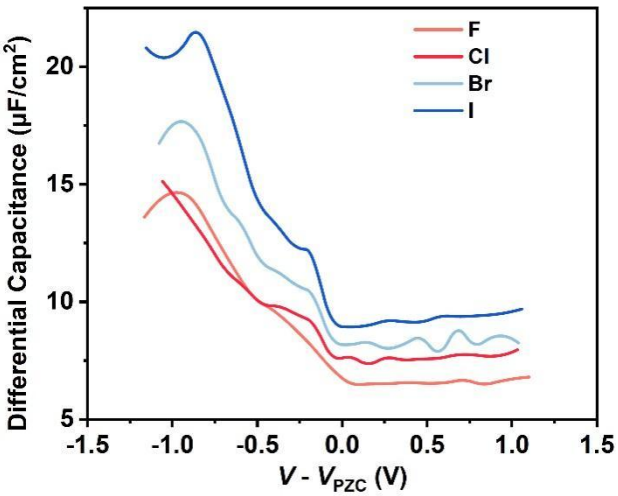

Supplementary Figure 1. Differential capacitance of Mo_2CT_x (T = F, Cl, Br, I, O) MXene.

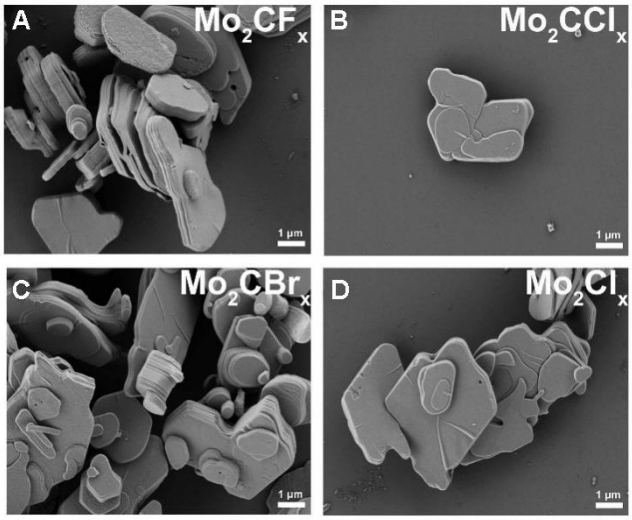

Supplementary Figure 2. SEM images of Mo_2CT_x (T = F, Cl, Br, I). (A) Mo_2CF_x. (B) Mo_2CCl_x. (C) Mo_2CBr_x. (D) Mo_2CI_x.

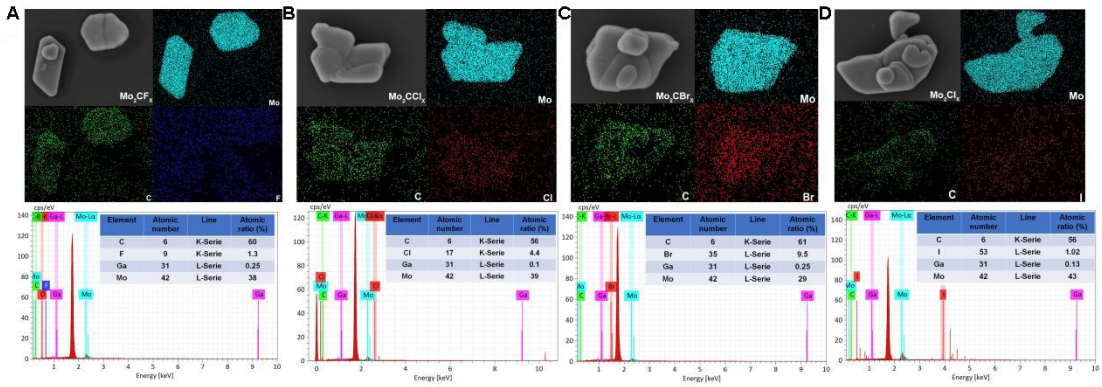

Supplementary Figure 3. EDS elemental distribution analysis on Mo_2CT_x (T = F, Cl, Br, I). (A) Mo_2CF_x. (B) Mo_2CCl_x. (C) Mo_2CBr_x. (D) Mo_2CI_x.

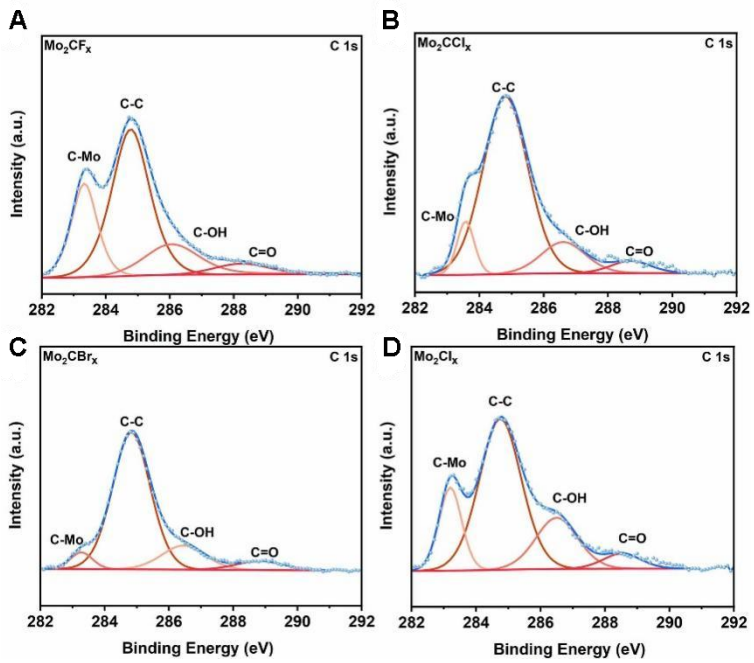

Supplementary Figure 4. XPS spectrum of C 1s for Mo_2CT_x (T = F, Cl, Br, I). (A) Mo_2CF_x. (B) Mo_2CCl_x. (C) Mo_2CBr_x. (D) Mo_2CI_x.

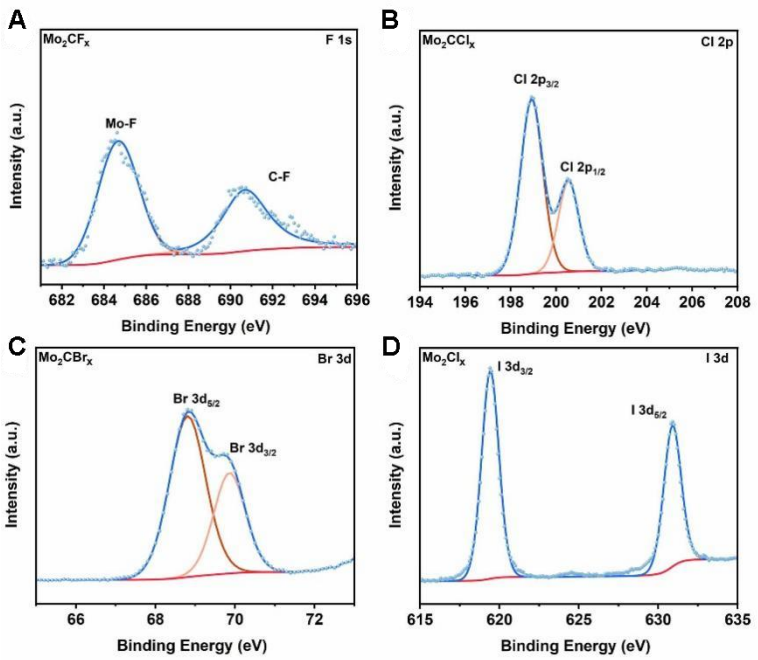

Supplementary Figure 5. XPS spectrum of surface termination for Mo_2CT_x (T = F, Cl, Br, I). (A) F 1s for Mo_2CF_x. (B) Cl 2p for Mo_2CCl_x. (C) Br 3d for Mo_2CBr_x. (D) I 3d for Mo_2CI_x.

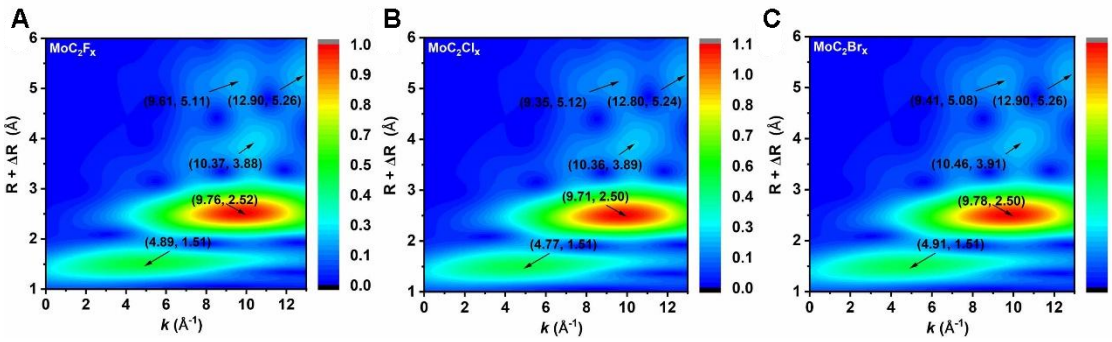

Supplementary Figure 6. Wavelet transform (WT) of Mo_2CT_x (T = F, Cl, Br, I). (A) Mo_2CF_x. (B) Mo_2CCl_x. (C) Mo_2CBr_x. (D) Mo_2CI_x.

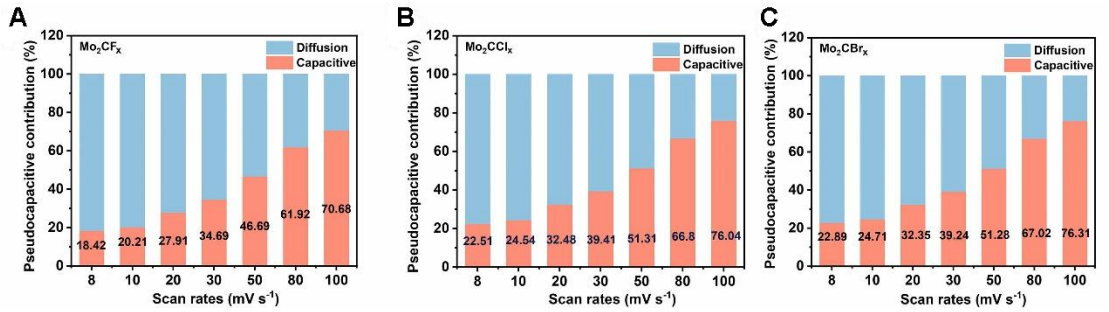

Supplementary Figure 7. The calculated diffusion and capacitive ratios at different scan rates for Mo_2CT_x (T = F, Cl, Br). (A) Mo_2CF_x. (B) Mo_2CCl_x. (C) Mo_2CBr_x.

REFERENCES

(1) Ravel, B.; Newville, M. ATHENA, ARTEMIS, HEPHAESTUS: data analysis for X-ray absorption spectroscopy using IFEFFIT. *J. Synchrot. Radiat.* **2005**, *12*, 537-541.

(2) Hafner, J. Ab-initio simulations of materials using VASP: Density-functional theory and beyond. *J Comput Chem* **2008**, *29*, 2044-2078.

(3) Letchworth-Weaver, K.; Arias, T. A. Joint density functional theory of the electrode-electrolyte interface: Application to fixed electrode potentials, interfacial capacitances, and potentials of zero charge. *Phys. Rev. B* **2012**, *86*, 075140.

(4) Zhan, C.; Zhang, P.; Dai, S.; Jiang, D.-e. Boron supercapacitors. *ACS Energy Lett.* **2016**, *1*, 1241-1246.

(5) Zhan, C.; Jiang, D. E. Contribution of dielectric screening to the total capacitance of few-layer graphene electrodes. *J Phys Chem Lett* **2016**, *7*, 789-794.

(6) Perdew, J. P.; Burke, K.; Ernzerhof, M. Generalized gradient approximation made simple. *Phys. Rev. Lett.* **1996**, *77*, 3865.

(7) Blochl, P. E. Projector augmented-wave method. *Phys Rev B Condens Matter* **1994**, *50*, 17953-17979.

(8) Sundararaman, R.; Goddard, W. A., 3rd. The charge-asymmetric nonlocally determined local-electric (CANDLE) solvation model. *J Chem Phys* **2015**, *142*, 064107.

(9) Zhan, C.; Neal, J.; Wu, J.; Jiang, D.-e. Quantum effects on the capacitance of graphene-based electrodes. *J. Phys. Chem. C* **2015**, *119*, 22297-22303.

(10) Shimada, T.; Takenaka, N.; Ando, Y.; Otani, M.; Okubo, M.; Yamada, A. Relationship between electric double-layer structure of MXene electrode and its surface functional groups. *Chem. Mater.* **2022**, *34*, 2069-2075.

(11) Zhan, C.; Zhang, Y.; Cummings, P. T.; Jiang, D. E. Enhancing graphene capacitance by nitrogen: effects of doping configuration and concentration. *Phys Chem Chem Phys* **2016**, *18*, 4668-4674.